PHENIX Results of Three-Particle Bose–Einstein Correlations in $\sqrt{s_{NN}} = 200$ GeV Au+Au Collisions

Tamás Novák

Eszterháy Károly University Károly Róbert Campus, H-3200 Gyöngyös, Mátrai út 36, Hungary
* Correspondence: novak.tamas@uni-eszterhazy.hu; Tel.: +36-37-518-300

Abstract: Bose–Einstein correlations (BECs) of identical hadrons reveal information about hadron creation from the strongly interacting matter formed in ultrarelativistic heavy-ion collisions. The measurement of three-particle correlations may in particular shed light on hadron creation mechanisms beyond thermal/chaotic emission. In this paper, we show the status of PHENIX measurements of three-pion correlations as a function of momentum differences within the triplets. We analyze the shape of the correlation functions through the assumption of Lévy sources and a proper treatment of the Coulomb interaction within the triplets. We measure the three-particle correlation strength (λ_3), which, together with the two-particle correlation strength λ_2, encodes information about hadron creation mechanisms. From a consistent analysis of two- and three-particle correlation strengths, we establish a new experimental measure of thermalization and coherence in the source.

Keywords: RHIC; PHENIX; Bose–Einstein correlations; Lévy distribution; thermalization; coherence

1. Introduction

In particle and nuclear physics, intensity interferometry provides a direct experimental method for the determination of sizes, shapes and lifetimes of particle-emitting sources (for reviews, see [1–5]). In particular, boson interferometry provides a powerful tool for the investigation of the spacetime structure of particle production processes, as Bose–Einstein correlations (BECs) of two or three identical bosons reflect both geometrical and dynamical properties of the particle-radiating source.

The size (radius) of the source in heavy-ion collisions has been found to decrease with increasing transverse momentum, p_t, or transverse mass, $m_t = \sqrt{m^2 + p_t^2}$, of the bosons. This effect can also be explained by hydrodynamical models [6,7]. The main purpose of the present paper is to determine the three-particle correlation strength (λ_3) as a function of transverse momentum. Recently [8], the two-particle correlation strength (λ_2) was determined. These measurements of λ_2, when combined with this analysis, may test the limits of the core–halo model [9–11] with a thermalized core. For this purpose, we introduce a new parameter, κ_3, which is a function of λ_3 and λ_2. This new parameter is not equal to 1 when there are extra effects in the core, for example, a core not fully thermalized, or when there is partial coherence in the core. The main purpose of the present work is to investigate whether κ_3 indicates extra effects or not.

We start with the definition of the three-particle correlation function:

$$C_3(\boldsymbol{k_1}, \boldsymbol{k_2}, \boldsymbol{k_3}) = \frac{N_3(\boldsymbol{k_1}, \boldsymbol{k_2}, \boldsymbol{k_3})}{N_1(\boldsymbol{k_1})N_1(\boldsymbol{k_2})N_1(\boldsymbol{k_3})} \tag{1}$$

where N_3 is the three-particle invariant momentum distribution, defined by

$$N_3(\boldsymbol{k_1}, \boldsymbol{k_2}, \boldsymbol{k_3}) = \int \mathcal{S}(\boldsymbol{r_1}, \boldsymbol{k_1})\mathcal{S}(\boldsymbol{r_2}, \boldsymbol{k_2})\mathcal{S}(\boldsymbol{r_3}, \boldsymbol{k_3})|\Psi_{\boldsymbol{k_1}, \boldsymbol{k_2}, \boldsymbol{k_3}}(\boldsymbol{r_1}, \boldsymbol{r_2}, \boldsymbol{r_3})|^2 \Pi_{i=0}^{3} d^4 \boldsymbol{r_i} \tag{2}$$

and N_1 is the single-particle invariant momentum distribution, defined as

$$N_1(\boldsymbol{k}) = \int \mathcal{S}(\boldsymbol{r}_1, \boldsymbol{k}_1)|\Psi_{\boldsymbol{k}}(\boldsymbol{r}_1)|^2 d^4\boldsymbol{r} \tag{3}$$

In the above equations, Ψ_{k_1,k_2,k_3} is the three-particle wave function, and Ψ_k is the single-particle wave function. Furthermore, $S(\boldsymbol{r}, \boldsymbol{k})$ is the source distribution, which describes the probability density of particle creation at the spacetime point $\boldsymbol{r}$ with momentum $\boldsymbol{k}$.

Our assumption for the source function is the symmetric Lévy distribution [12–16], which is defined by

$$L(\alpha, R, \boldsymbol{r}) = \frac{1}{(2\pi)^3} \int d^3\boldsymbol{q}\, e^{i\boldsymbol{q}\boldsymbol{r}} e^{-\frac{1}{2}|qR|^{\alpha}} \tag{4}$$

where α is the Lévy index, and R is the Lévy scale. Then $\alpha = 2$ gives back the Gaussian case, and $\alpha = 1$ yields a Cauchy distribution. For the Lévy stable source distribution, $0 < \alpha \le 2$ in general.

Assuming properly symmetrized plane-waves for the wave functions and the Lévy distribution as the source function, the three-particle correlation function is given as

$$C_3^{(0)}(k_{12}, k_{13}, k_{23}) = 1 + \ell_3 e^{-0.5(|2k_{12}R|^{\alpha} + |2k_{13}R|^{\alpha} + |2k_{23}R|^{\alpha})} + \ell_2 \left(e^{|2k_{12}R|^{\alpha}} + e^{|2k_{13}R|^{\alpha}} + e^{|2k_{23}R|^{\alpha}} \right) \tag{5}$$

where $k_{ij} = |\boldsymbol{k}_i - \boldsymbol{k}_j|/2$, that is, the half-momentum difference of the ith and jth particles. Furthermore, the ℓ_2 parameter is the two-particle correlation strength parameter in the three-particle correlation function, and ℓ_3 is the three-particle strength parameter.

To be able to fit the model to the data, the correlation function has to be completed with a background that parameterizes possible long-range correlations. In this analysis, we use a simple linear background in every direction, with the same slope. Thus the correlation function is the following:

$$C_{3,\text{fit}}^{(0)}(k_{12}, k_{13}, k_{23}) = N(1 + \epsilon k_{12})(1 + \epsilon k_{13})(1 + \epsilon k_{23})C_3^{(0)}(k_{12}, k_{13}, k_{23}) \tag{6}$$

We also have to take into account the Coulomb interaction, as this decreases the number of particle pairs at low-momentum differences. To add Coulomb correction to the model, we define a Coulomb correction factor:

$$K_3(\boldsymbol{k_{12}}, \boldsymbol{k_{23}}, \boldsymbol{k_{31}}) = \frac{\int d^3\boldsymbol{r_1} d^3\boldsymbol{r_2} d^3\boldsymbol{r_3} \mathcal{S}(\boldsymbol{r_1}) \mathcal{S}(\boldsymbol{r_2}) \mathcal{S}(\boldsymbol{r_3}) |\Psi_{k_{12},k_{23},k_{31}}^0(\boldsymbol{r_1}, \boldsymbol{r_2}, \boldsymbol{r_3})|^2}{\int d^3\boldsymbol{r_1} d^3\boldsymbol{r_2} d^3\boldsymbol{r_3} \mathcal{S}(\boldsymbol{r_1}) \mathcal{S}(\boldsymbol{r_2}) \mathcal{S}(\boldsymbol{r_3}) |\Psi_{k_{12},k_{23},k_{31}}^C(\boldsymbol{r_1}, \boldsymbol{r_2}, \boldsymbol{r_3})|^2} \tag{7}$$

where Ψ^0 is the free-particle wave function (symmetrized plane wave), and Ψ^C is the (symmetrized) solution of the full three-particle Coulomb problem. Instead of solving the three-particle Coulomb problem, we use a general approach to handle the three-particle Coulomb interaction, which is called the "Generalized Riverside" method [17]:

$$K_3(k_{12}, k_{13}, k_{23}) \approx K_2(k_{12})K_2(k_{13})K_2(k_{23}), \quad \text{with} \quad K_2(k_{ij}) = \frac{\int d^3\boldsymbol{r_1} d^3\boldsymbol{r_2} \mathcal{S}(\boldsymbol{r_1}) \mathcal{S}(\boldsymbol{r_2}) |\Psi_{k_{12}}^0(\boldsymbol{r_1}, \boldsymbol{r_2})|^2}{\int d^3\boldsymbol{r_1} d^3\boldsymbol{r_2} \mathcal{S}(\boldsymbol{r_1}) \mathcal{S}(\boldsymbol{r_2}) |\Psi_{k_{12}}^C(\boldsymbol{r_1}, \boldsymbol{r_2})|^2} \tag{8}$$

This approximates the three-particle Coulomb correction well if certain conditions [17] are satisfied, and it does not depend on the directions of the momentum differences, only their magnitude. With this Coulomb correction factor, the full BEC function is

$$C_3(k_{12}, k_{13}, k_{23}) = C_{3,\text{fit}}^{(0)}(k_{12}, k_{13}, k_{23})K_{Coulomb}(k_{12}, k_{13}, k_{23}) \tag{9}$$

By using this approximation, we are able to reuse the Coulomb correction calculation method developed in [18]. After some consistency checks, we conclude that using this approximation can be considered, as the relative systematic error due to this approximation is less than 2%.

The two- and three-particle correlation strengths are defined as the extrapolated intercept of the given correlation function:

$$\lambda_2 \equiv C_2(k_{12} \to 0) - 1 \tag{10}$$

$$\lambda_3 \equiv C_3(k_{12} = k_{13} = k_{23} \to 0) - 1 \tag{11}$$

With respect to these, it is important to note that not all pions are created directly from the strongly interacting matter. A significant fraction of pions are secondary, coming from decays. Hence the source will have two components: a core of primordial pions, and a halo consisting of the decay products of long-lived resonances (such as η, η', K_s^0, and ω):

$$S = S_{core} + S_{halo} \tag{12}$$

In the core–halo model, the fraction of the core is defined by

$$f_c = \frac{N_{\text{core}}}{N_{\text{core}} + N_{\text{halo}}} \tag{13}$$

where N_{core} is the number of pions in the core, and N_{halo} is the number of pions in the halo. If there is partial coherence in the core, a coherence parameter can be introduced [19,20], examining the fraction of coherently produced pions in the core:

$$p_c = \frac{N_{\text{coherent}}}{N_{\text{coherent}} + N_{\text{incoherent}}} \tag{14}$$

where $N_{\text{coherent}} + N_{\text{incoherent}} = N_{\text{core}}$. With these, λ_2 and λ_3 can be expressed as functions of f_c and p_c:

$$\lambda_2 = f_C^2 \left[(1 - p_c)^2 + 2p_c(1 - p_c) \right] \tag{15}$$

$$\lambda_3 = 2f_C^3 \left[(1 - p_c)^3 + 3p_c(1 - p_c)^2 \right] + 3f_C^2 \left[(1 - p_c)^2 + 2p_c(1 - p_c) \right] \tag{16}$$

To be able to investigate the partial coherence within the limits of this model, we have to take Equations (15)–(16) and use the measured λ_2 and λ_3 parameters as input in these equations; we also have to look for f_c and p_c values that solve both equations. To determine whether a solution exists, we can plot f_c as a function of p_c with given λ_2 and λ_3. In this way, we obtain two curves (one from the equation with λ_2, and the other from the equation with λ_3), and if these curves overlap, then the second- and third-order BEC functions are consistent with each other, and the degree of partial coherence can be determined from the region of the overlap.

2. Results

The data used in the analyses were collected by the PHENIX detector in 2010; 7.3 billion minimum bias Au+Au collisions at $\sqrt{s_{NN}} = 200$ GeV were recorded. We measured three-particle correlation functions of $\pi^- \pi^- \pi^-$ and $\pi^+ \pi^+ \pi^+$ triplets in 31 m_T bins ranging from 228 to 871 MeV, with event selection, single track cuts and pair cuts identical to the analysis of [8]. The visualization of three-dimensional fits is difficult; thus instead of showing two-dimensional projections of these three-dimensional fits, we have decided to show, as an illustration, various one-plus-one dimensional slices of them. These slices were obtained by requiring that the two-particle relative momenta $k_{i,j}$ between the pairs $(i, j) = (1,2)$, $(2,3)$ and $(3,1)$ were equal. The χ^2/NDF values and the confidence levels were statistically acceptable. Figure 1 indicates the PHENIX preliminary three-particle correlation data and the fitted curve as a univariate slice of a multi-variate function. We note that no significant long-range correlation was observed: ϵ was close to zero. In these fits, the values of

the Lévy scale R and the Lévy index of stability α were taken from PHENIX preliminary two-particle correlation data in the same transverse-momentum bins and in the same selection of minimum-bias $\sqrt{s_{NN}} = 200$ GeV Au+Au collisions. (See these preliminary R and α data in [21].) Within one standard deviation, the same parameter values were obtained if we released the values of R and α in these fits, indicating an internal consistency between the two- and three-particle correlation measurements. Given this internal consistency and our focus on the comparison of the strength or intercept parameters λ_2 and λ_3 of the two- and three-particle BEC functions, here we report these values using the R and α values as determined from the two-particle BEC function measurements in minimum-bias $\sqrt{s_{NN}} = 200$ GeV Au+Au collisions [21].
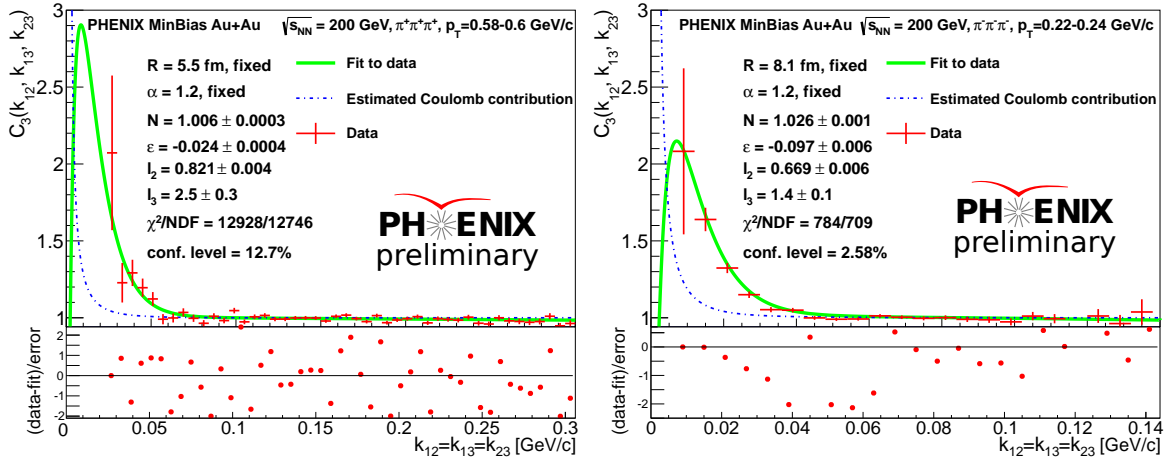
Figure 1. Diagonal visualization of the three-particle Bose–Einstein correlation functions C_3 with the results of fits.

2.1. Three-Particle Correlation Strength

The three-particle correlation strength, derived from ℓ_2 and ℓ_3 fit parameters as $\lambda_3 = \ell_2 + \ell_3$, can be seen in Figure 2. According to the core–halo model, λ_3 had to be in the range $[0, 5]$, as indicated by a green box in Figure 2. One can see that within errors, this parameter fell in the allowed range. The detailed description of the systematic uncertainty sources is given in [8].
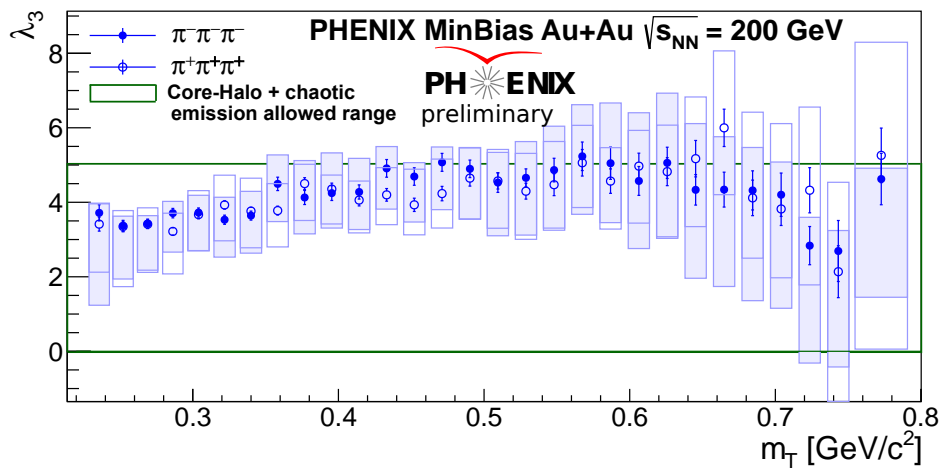
Figure 2. The three-particle correlation strength, λ_3, as a function of m_T. Statistical and systematic uncertainties are shown as bars and boxes, respectively.
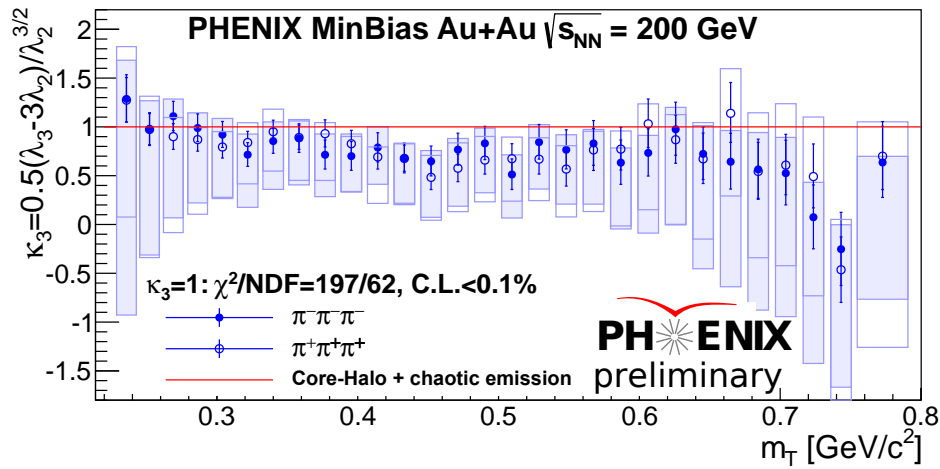
2.2. Core–Halo Independent Parameter

In this subsection, the possibility of partial coherence is investigated. We introduce a new parameter, a combination of λ_3 and λ_2, as follows:

$$\kappa_3 = \frac{\lambda_3 - 3\lambda_2}{2\sqrt{\lambda_2^3}} \tag{17}$$

This parameter does not depend on the value f_c, and its value is unity independently of the transverse mass, if the particle emission has no coherent component or if $p_c = 0$ in the core–halo picture of n-particle BECs.

The measured κ_3 parameter is shown in Figure 3 and was calculated by using λ_3 from the fits described in this paper, and λ_2 from [21]. Our errors were still preliminary, and a full systematic analysis is in progress. Figure 3 shows the κ_3 parameter for the average m_T of the triplets.

Figure 3. Core–halo independent parameter as a function of m_T. Statistical and preliminary systematic uncertainties are shown as bars and boxes, respectively.

We observe that κ_3 was different from unity at $m_T \approx 450$ MeV. The deviation of κ_3 from 1 may indicate some kind of partial coherence; however, the preliminary status of these data points and their error bars prevent us from a more definitive conclusion. Further investigations are ongoing and will be reported elsewhere. Figure 4 shows f_c as a function of p_c for different m_T regions. Here we took Equations (15)–(16) and the measured λ_2 and λ_3 parameters and determined the allowed (f_c, p_c) region, as shown in Figure 4.
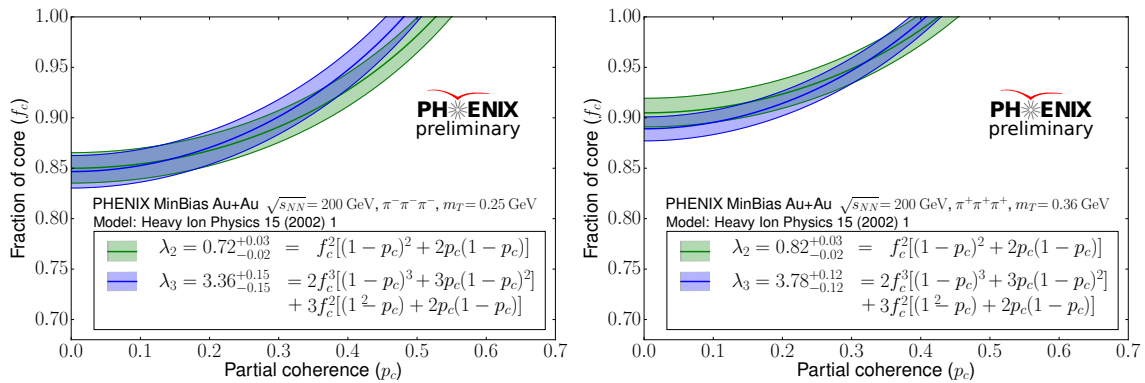
Figure 4. The fraction of the core f_c parameter as a function of coherence parameter p_c for two different m_T values.

3. Conclusions

In this paper, we simultaneously investigated two- and three-particle femtoscopic correlation functions in PHENIX Au+Au collisions at 200 GeV/nucleon collision energy. Lévy distributions yielded correlation functions that provide a statistically acceptable description of the measurements. In this paper, we used the source parameters R and α from two-particle fits and obtained the three-particle correlation strength from the analysis of three-particle correlations. We have investigated the results in view of the core–halo model and derived a core–halo independent parameter κ_3. These preliminary results have been compared to predictions based on chaotic emission, and very small deviations were observed. This, however, needs a detailed final analysis, which we plan to carry out in the near future.

Conflicts of Interest: The authors declare no conflict of interest.

References

1. Gyulassy, M.; Kauffmann, S.K.; Wilson, L.W. Pion interferometry of nuclear collisions. *Phys. Rev. C* **1979**, *20*, 2267–2292.
2. Boal, D.H.; Gelbke, C.K.; Jennings, B.K. Intensity interferometry in subatomic physics. *Rev. Mod. Phys.* **1990**, *62*, 553–602.
3. Baym, G. The physics of Hanbury Brown-Twiss intensity interferometry: From stars to nuclear collisions. *Acta Phys. Pol. B* **1998**, *29*, 1839–1884.
4. Kittel, W. Bose-Einstein Correlations in Z Fragmentation and Other Reactions. *Acta Phys. Pol. B* **2001**, *32*, 3927–3972.
5. Csörgő, T. Particle Interferometry from 40 MeV to 40 TeV. *Heavy Ion Phys.* **2002**, *15*, 1–80.
6. Wiedemann, U.; Scotto, P.; Heinz, U. Transverse momentum dependence of Hanbury-Brown-Twiss correlation radii. *Phys. Rev. C* **1996**, *53*, 918–931.
7. Csörgő, T.; Lörstad, B. Bose-Einstein correlations for three-dimensionally expanding, cylindrically symmetric, finite systems. *Phys. Rev. C* **1996**, *54*, 1390–1403.
8. Adare, A.; Aidala, C.; Ajitanand, N.N.; Akiba, Y.; Akimoto, R.; Alexander, J.; Alfred, M.; Al-Ta'ani, H.; Angerami, A.; Aoki, K.; et al. Lévy-stable two-pion Bose-Einstein correlations in $\sqrt{s_{NN}} = 200$ GeV Au+Au collisions. *arXiv* **2017**, arXiv:nucl-ex/1709.05649.
9. Bolz, J.; Ornik, U.; Plumer, M.; Schlei, B.R.; Weiner, R.M. Resonance decays and partial coherence in Bose-Einstein correlations. *Phys. Rev. D* **1993**, *47*, 3860–3870.
10. Csörgő, T.; Lörstad, B.; Zimányi, J. Bose-Einstein correlations for systems with large halo. *Z. Phys. C* **1996**, *71*, 491–497.
11. Csanád, M. Measurement and analysis of two- and three-particle correlations. *Nucl. Phys. A* **2006**, *774*, 611–614.
12. Nolan, J.P. Univariate Stable Distributions. In *Stable Distributions—Models for Heavy Tailed Data*; Publishing House: Boston, MA, USA, 2018.
13. Metzler, R.; Barkai, E.; Klafter, J. Anomalous Diffusion and Relaxation Close to Thermal Equilibrium: A Fractional Fokker-Planck Equation Approach. *Phys. Rev. Lett.* **1999**, *82*, 3563–3567.
14. Csörgő, T.; Hegyi, S.; Zajc, W.A. Bose-Einstein Correlations for Levy stable source distributions. *Eur. Phys. J. C* **2004**, *36*, 67–78.
15. Csanád, M.; Csörgő, T.; Nagy, M. Anomalous diffusion of pions at RHIC. *Braz. J. Phys.* **2007**, *37*, 1002–1013.
16. Csanád, M. Lévy femtoscopy with PHENIX at RHIC. *Universe* **2017**, *3*, 85.
17. Gangadharan, D. Techniques for multiboson interferometry. *Phys. Rev. C* **2015**, *92*, 014902.
18. Alt, E.O.; Csörgő, T.; Lörstad, B.; Schmidt-Sorensen, J. Coulomb corrections to the three-body correlation function in high-energy heavy ion reactions. *Phys. Lett. B* **1999**, *458*, 407–414.

19. Boggild, H.; Boissevainb, J.; Doddc, J.; Esumid, S.; Fabjane, C.W.; Ferencef, D.; Franzg, A.; Hardtkeh, D.; van Heckeb, H.; Humanich, T.J.; et al. Three pion correlations in sulphur lead collisions at the CERN SPS. *Phys. Lett. B* **1999**, *455*, 77–83.

20. Csörgő, T.; Lörstad, B.; Schmid-Sørensen, J.; Ster, A. Partial coherence in the core–halo picture of Bose–Einstein n-particle correlations. *Eur. Phys. J. C* **1999**, *9*, 275–281.

21. Kincses, D.; PHENIX Collaboration. PHENIX results on Lévy analysis of Bose-Einstein correlation functions. *Acta Phys. Polon. Supp.* **2017**, *10*, 627.